Improvisations in phototrophy. Protein engineering and functional investigation of rhodopsin proton-pumps

Ganapathy, S.

Chapter 2

Retinal analogs can modulate the spectral properties and proton pumping of PR and GR

Proteorhodopsins bind all-*trans* retinal A1 as a native ligand to absorb visible light (520-540 nm). Here, we describe the modulation of the absorbance band of Monterey Bay proteorhodopsin (PR), its red-shifted double mutant PR-D212N-F234S and *Gloeobacter* rhodopsin (GR). This was approached using three analogs of all-*trans* retinal A1, which differ in their electronic and conformational properties. We further probed the effect of these retinal analogs on the proton pump activity of the pigments. Our results indicate that, while the constraints of the retinal binding pocket differ for the proteorhodopsins, at least two of the retinal analogs are capable of shifting the absorbance bands of the pigments either bathochromically or hypsochromically, while maintaining their proton pump activity. Furthermore, the shifts implemented by the analogs add up to the shift induced by the double mutation in PR-DNFS. This type of chromophore substitution may present attractive biotechnological applications.

This chapter is published as: S. Ganapathy, O. Bécheau, H. Venselaar, S. Frölich, J. B. van der Steen, Q. Chen, S. Radwan, J. Lugtenburg, K. J. Hellingwerf, H. J. M. de Groot, W. J. de Grip **(2015)** *Biochemical Journal* 467: 333-343

2.1 Introduction

In this chapter, we investigate the effects of three retinal analogs, which differ in their electronic and conformational properties, on the action spectrum of wild type (WT) PR and GR and the red-shifted double mutant PR-D212N-F234S (PR-DNFS) [1]. The three all-*trans* analogs of the native retinal A1 are: retinal A2, Phe-retinal A1 and 6-s-*trans* locked retinal A1 (Figure 2.1). Retinal A2 has the same structural make-up as retinal A1, but contains an elongated π-conjugated polyene chain. This analog has been shown to red-shift the absorbance band of archaeal rhodopsins [2-5] and xanthorhodopsin (XR) [6]. We anticipated that this analog would have a similar effect on the proteorhodopsins. Phe-retinal A1 contains an even more complex conjugated system, but lacks the methyl groups in the ring element. This analog blue-shifts the absorbance band of bR [7, 8] and XR [6, 9]. In 6-s-*trans* locked retinal A1, the C6-C7 bond is locked in an s-*trans* configuration. The use of this analog corroborated evidence that the chromophore in bR and XR contains a 6-s-*trans* configuration [10]. Our results show that retinal analogs can significantly modulate the spectral properties of proteorhodopsins with at least partial preservation of proton pump activity, and that the binding pocket constraints differ for PR and GR. Further, we show that in PR-DNFS, the analog-induced spectral shifts are additive to the mutation-induced shift.

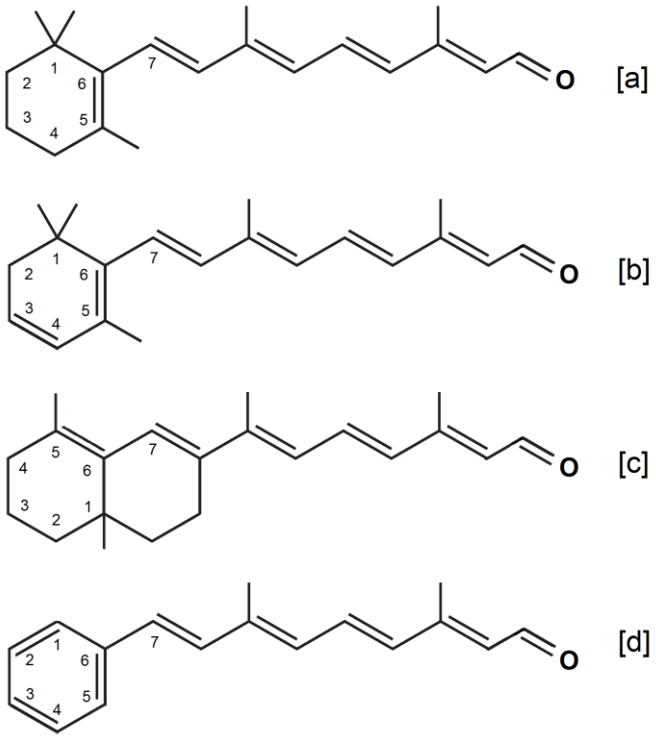

Figure 2.1 Chemical structures of retinal analogs used in this chapter [a] A1 [b] A2 [c] ALL-E [d] PHE. For spectral properties, see the Appendix figure A.2.

2.2 Experimental section

2.2.1 Materials:

E. coli strain UT5600 and the pKJ900 plasmids encoding PR or GR with a C-terminal 6-His tag were a generous gift from Dr. K. Jung, University of Seoul, South Korea [1]. UT5600 was used to express the recombinant proteins. All-*trans* retinal A1 (hereafter called A1) was obtained from Sigma-Aldrich. All-*trans* retinal A2 (A2) and all-E-6-s-*trans* locked retinal A1 (ALL-E) were prepared as described before [10, 11]. All-*trans*-phe-retinal A1 (PHE) was synthetized in analogy to A1 and A2, but starting from benzaldehyde, and the structure was confirmed by ^{1}H NMR [36]. The source of all other chemicals is outlined in the appendix (A.1)

2.2.2 Site-directed mutagenesis:

Site directed mutagenesis was performed on the PR gene using mis-match PCR. In brief, the pKJ900 plasmid containing PR was linearized by restriction with Esp3I and subjected to mis-match PCR using overlapping primers containing the corresponding mutation sites for the D212N and the F234S mutations. 25 cycles of PCR were run at 95°C for 30 s, 55°C for 30 s and 68°C for 60 s. The mutant gene was further amplified using outside vector primers with the same PCR program. The sequences of the primers are listed in the appendix (A.4). The amplified mutant gene and vector were restricted at HindIII and XbaI sites and run on an agarose gel. The bands corresponding to the restricted mutant gene and the empty vector were cut out, extracted using a Qiagen gel extraction kit and ligated overnight at 4°C. The ligated plasmid was then transformed into *E. coli* UT5600 made chemically competent using calcium chloride.

2.2.3 Bacterial cell culturing:

The cells were grown in LB medium with 50 μg/mL ampicillin at 30°C in an orbital shaker at 180 rpm. Overnight cultures were grown from frozen glycerol stocks of transformed cells, which were diluted 1:100 to get the working culture. At a cell density corresponding to an OD_{600} of 0.3-0.4, expression of the opsin was induced by the addition of isopropyl β-D-1-thiogalactopyranoside (IPTG) to a final concentration of 1 mM. The cells were allowed to grow further for 24 h at 30°C and then harvested.

2.2.4 Regeneration of proteo-opsin with retinal:

Retinals were stored at -80°C in hexane stock solutions, with the exception of PHE which was stored in methanol. The absorbance spectra and λ_{max} of the retinal analogs are presented in the appendix (A.2). The molar absorbance of A1 and A2 were taken as 49000 and 44000 $M^{-1}cm^{-1}$ respectively [12, 13]. The molar absorbance of ALL-E and PHE were

assumed to be similar to that of A1. At the time of use, the required aliquot of stock solution was evaporated and the residue re-dissolved in dimethylformamide (DMF) to obtain a concentration of 1 mM. This solution was then added to a crude cellular lysate or to isolated membrane vesicles containing the opsin to achieve a final retinal concentration of 5-10 µM, and incubated under dim light for up to 60 min at room temperature (RT) or, if necessary, overnight at 4°C.

2.2.5 Preparation and analysis of membrane vesicles:

The cells were harvested by centrifugation (3200xg, 20 min, RT), and the pellet was resuspended in an ice-cold solution of 50 mM Tris-HCl, 150 mM NaCl, pH 7 (10 mL per 50 mL of culture). The suspended cells were lysed by sonication at 4°C using a Sonics vibra-cell sonicator (10 min, 4 s pulses, 5 s pauses, 25% amplitude) and centrifuged to remove insoluble material and cellular debris (4000xg, 15 min, 4°C). The resulting supernatant with membrane vesicles was incubated with the selected retinal for one hour at RT and the vesicles were then pelleted by high-speed centrifugation (147,000xg, 1 h, 4°C). The pellet was resuspended in 150 mM NaCl (2 mL per 50 ml culture). For solubilisation of membrane proteins, DDM was added to a final concentration of 2% (w/v), and the suspension was incubated with shaking for an hour at 4°C, followed by overnight incubation at 4°C. The insoluble material was removed by centrifugation (16,000xg, 20 min, 4°C). The supernatant was used for spectral analysis.

2.2.6 Proteorhodopsin purification:

The cell pellet was resuspended in ice cold lysis buffer (5 ml/100 ml culture volume) containing 20 mM Tris, 50 mM NaCl, 20 mM imidazole, 0.1% DDM, pH 7, supplemented with an EDTA-free protease inhibitor tablet, benzonase (4 units/100 mL culture) and lysozyme (4 mg/100 mL culture). The suspension was sonicated at 4°C and centrifuged to remove cellular debris as described in the previous section. At this stage, the crude

mixture was incubated with the selected retinal for one hour at RT. DDM was then added to a final concentration of 1.5% (w/v) and the sample was kept rotating overnight at 4°C. The insoluble material was removed by centrifugation (4,000xg, 25 min, 4°C) and the resulting supernatant was utilized as a crude extract. For purification of the His-tagged proteorhodopsins, immobilized-metal affinity chromatography (IMAC) was exploited using 0.4 mL Ni^{2+}-NTA resin per 100 mL original culture volume. The resin was contained in a spin column and first equilibrated with buffer A (20 mM bis-tris propane, 0.5 M NaCl, 0.1% DDM, pH 8) containing 20 mM imidazole. The crude extract was then allowed to equilibrate with the column for 15 min at RT. The column was washed 5 times with 5 column volumes of buffer A containing 50 mM imidazole at RT. Finally, strongly bound protein was eluted using buffer A containing 250 mM imidazole and 0.01% DDM at RT. Fractions of 0.3 mL were collected. Fractions containing the purified proteorhodopsin were combined and analyzed by spectroscopy and SDS-PAGE. Thus purified proteorhodopsin could be stored at 4°C for several weeks, but was kept at -80 °C for long-term storage.

2.2.7 Spectroscopy:

The spectral properties of all samples were measured using a Shimadzu UV-Vis spectrophotometer (UV-1601). The pH-dependence of the main absorbance band of the proteorhodopsins was assessed in solubilised membrane vesicles at different pH values by diluting the samples 1:1 with buffers containing either 100 mM bis-tris-propane at pH 6.5 or 9.5, or 20 mM MES at pH 5. To isolate the major absorbance band of the proteorhodopsin out of the composite spectrum of membrane vesicles, hydroxylamine was added from a 1 M stock solution, pH 7, to a final concentration of 50 mM, followed by incubation at RT under ambient light. Hydroxylamine attacks the Schiff base and releases the retinal from the opsin binding pocket as retinaloxime. A difference spectrum then reveals

the major absorbance band of the proteorhodopsin present. Absorbance maxima were determined using the internal peak-pick function of the software UVProbe.

2.2.8 SDS-PAGE:

The crude and purified protein fractions were analysed by SDS-PAGE. In brief, aliquots of the samples were diluted with SDS sample buffer, incubated for 30 min at 37°C, and run on a 12.5% polyacrylamide gel at 20 mA for 2 h. The gel was stained using Coomassie brilliant-blue G for 2 hours according to the manufacturer's instructions and destained overnight using MilliQ. Gel images were obtained using the Bio-Rad GS-800 gel imaging dock.

2.2.9 Starvation of cells:

Overnight cultures were diluted 1:100 times to get a working culture of 25 ml. At a cell density corresponding to an OD_{600} of 0.3-0.4, production of the proteorhodopsin was induced by the addition of IPTG to a final concentration of 1 mM and of the selected retinal to a final concentration of 5 µM. The cultures were allowed to grow for a further 24 h at 30°C in the dark, and then harvested. The cells were washed twice in starvation buffer (SB) containing 250 mM KCl, 10 mM NaCl, 10 mM $MgSO_4$, 100 µM $CaCl_2$, 10 mM Tris-HCl pH 7 and were starved by incubation with continuous mixing for 4 days at RT. The cells were washed another 3 times and resuspended in 5 ml SB supplemented with 40 µM final concentration of valinomycin. The cell suspension was incubated for 30 min in the dark at RT.

2.2.10 Proton pumping assay:

The cell suspension was illuminated through a bandpass filter in the range of 300-800 nm (BG-18, Schott) using a halogen light source with fibre optics (Euromex, LE.5211). A photon flux of 40 $\mu mol.m^{-2}.s^{-1}$ was used

throughout. Light-induced pH changes were measured with a pH microelectrode (SenTix MIC, WTW) and the readout was monitored by a pH meter (Inolab pH 7310, WTW) fed into a computer. The following light regime was used: 1 min dark, 1 min light, 2 min dark, 1 min light, 2 min dark. Pumping rates were calculated for 5 mL of the cell suspension using two independent trials. Finally, CCCP was added to a final concentration of 40 µM and the suspension was incubated at RT for half an hour in the dark. Light induced pH changes were then measured again using the same light regime. This system was calibrated using 0.1 M oxalic acid and 0.1 M HCl. Pumping rates were calculated as protons/sec from the initial rate of the light-induced pH change, if required corrected for baseline drift in controls (starved cells without expression of proteo-opsin or without retinal). Molecular pumping rates could subsequently be calculated after assay of the proteorhodopsin level (see below).

2.2.11 Determination of proteorhodopsin levels:

The above cell suspension from the proton pumping assay was rinsed with starvation buffer (2.2.9) and the pellet was resuspended in 10 ml buffer B (10mM Tris-Cl, 150 mm NaCl, pH 7). The cell suspension was sonicated as mentioned above and the membrane vesicles and cell debris were pelleted together (147,000xg, 4°C, 1 h). The pellet was resuspended in 1.5 ml of 150 mM NaCl. DDM was added to a final concentration of 2.5% and incubated at RT with mixing overnight. Under these conditions, maximal extraction of proteorhodopsin was achieved without significant losses. The following day, the insoluble material was removed by centrifugation (16,000xg, 4°C, 20 min). The supernatant was used to measure an absorbance spectrum before and after bleaching with hydroxylamine as described above. The optical density value at the absorbance maximum was used to calculate the original proteorhodopsin level in the cell suspension using a molar absorbance of 45000 $M^{-1}cm^{-1}$[14].

2.2.12 Construction of homology models:

A homology model for PR was built using the structure of sensory rhodopsin II (SRII) as a template (PDB 1H2S) [15], with which it has the highest sequence identity out of the retinal proteins for which structural information was available at that time (24% sequence identity). For GR, we built a model using the structure of XR as a template (PDB 3DDL, 56% sequence identity) [16]. Model building and subsequent analysis was performed using the WHAT IF (PMID:2268628) & YASARA (PMID:11948792) Twinset with standard parameters.

2.3 Results

2.3.1 Reconstitution of proteorhodopsins with retinal analogs:

Production of proteorhodopsins following induction with IPTG and simultaneous addition of A1 to the UT5600 cells could be easily verified by the red coloration of the pelleted cells or membrane vesicle preparation. However, this requires substantial amounts of retinal (up to 0.5 mg/100 mL culture) and in view of the limited quantities of retinal analogs available, we investigated other options. It turned out that the apoproteins produced *in vivo* would still readily bind A1 after harvesting the cells and preparation of membrane vesicles. We observed that incubation of these vesicles with A1 resulted in at least the same yield of pigment as when A1 was supplied to the cell culture, but required 5-10 fold less retinal. Incorporation of A1 or the analogs could be detected visually from the development of a red or purple color (Figure 2.2) and was subsequently characterized by spectroscopy after solubilization in 2% (w/v) DDM. Since the spectra also have contributions from other membrane components (cytochromes, excess retinal), the specific absorbance band of the proteo-rhodopsin was isolated by incubation with 50 mM hydroxylamine (Figure 2.2). This procedure works well for all proteorhodopsins tested. We

observed that the PRs were much more sensitive to bleaching with hydroxylamine than GR, which may be related to the slower photocycle kinetics of PR [17-19]. The absorbance maxima obtained with A1 at neutral pH for PR, PR-DNFS, and GR lie at 526 nm, 545 nm and 540 nm respectively, and are in good agreement with those reported in the literature [1, 18, 20].

Upon incubation of the three proteo-opsin species with the retinal analogs we observed that all three analogs regenerate the PR opsins with distinct absorbance maxima, while only two of the analogs regenerate the GR opsin (Figure 2.3). A2 and ALL-E were rapidly incorporated within 30-60 min at RT. Incorporation of PHE was much slower, requiring additional overnight incubation at 4°C. Incorporation of A2 induces an appreciable red-shift of about 30 nm relative to A1 in the absorbance band of all species tested. Incorporation of PHE on the other hand causes a significant blue-shift of about 30 nm in PR, while it does not seem to generate a stable pigment with GR. This was further corroborated by the lack of a distinct negative peak after hydroxylamine treatment of GR-opsin vesicles, incubated with PHE (data not shown). ALL-E can be incorporated in all three opsins, and produces only a small red-shift in their absorbance band, relative to A1.

The position of the absorbance band of PR and reported mutants is pH-dependent, probably because of protonation of D97 [14, 21], which induces a red-shift of 25-30 nm. The corresponding pKa values for PR and PR-DNFS are reported to be 7.3 and 8.0, respectively [1]. This strong pH dependence has not yet been observed for GR [18, 22, 23]. We were interested in whether the analog pigments would show a similar behaviour, and recorded the absorbance spectra of the corresponding solubilized membrane vesicles at pH 5, 6.5 and 9.5 (Table 2.1).

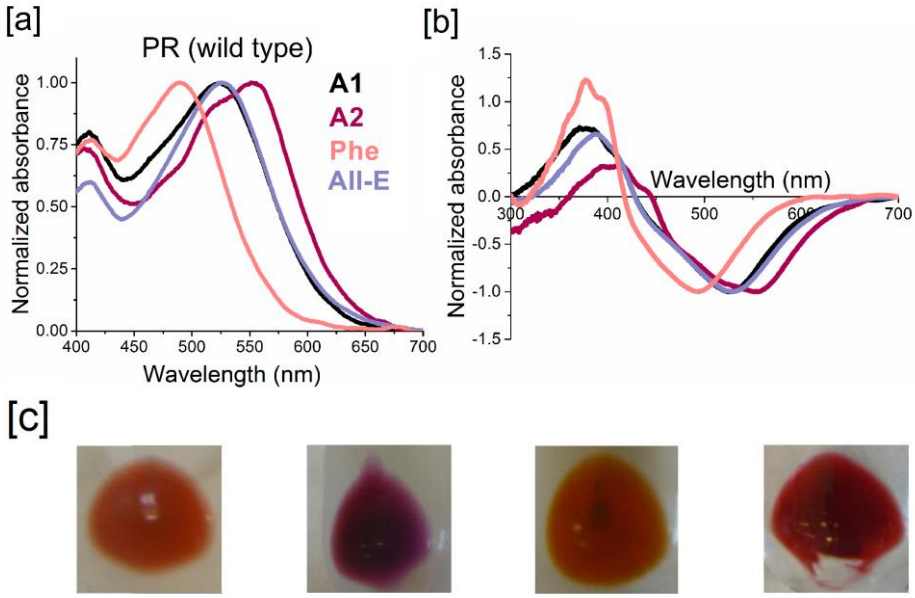

Figure 2.2 [a] Absorbance spectra of solubilized membrane vesicles containing PR reconstituted with the indicated retinals [b]. Difference spectra of the same obtained after incubation of with 50 mM hydroxylamine. Negative bands correspond to the original holoprotein absorbance band. [c] Coloured membrane vesicle pellets of A1, A2, PHE and ALL-E respectively.

All PR-based analog pigments showed a clear pH dependence of their visible absorbance band. The largest red shift upon going from pH 9.5 to 5 of around 25 nm was observed for the ALL-E analog of PR. The magnitude of the shift between pH 9.5 and 5 will also depend on the value of the pKa. On the other hand, we did not observe a significant pH effect in this range on the absorbance profile of GR nor of the GR-based analog pigments.

2.3.2 Purification of the proteorhodopsins:

Following their characterization in membrane vesicles, we aimed for optimal spectral characterization of the native and analog pigments by purification over a Ni^{2+}-NTA resin exploiting their C-terminal 6-His tag.

Species	Retinal analog	λmax (nm)		
		pH 9.5	pH 6.5	pH 5
PR	A1	516	526	531
	A2	551	553	570
	ALL-E	522	525	547
	PHE	478	490	495
PR-DNFS	A1	535	542	553
	A2	560	565	582
	ALL-E	541	547	560
	PHE	492	497	510
GR	A1	537	533	536
	A2	564	569	572
	ALL-E	541	538	546

Table 2.1 λ_{max} values of the pigments at pH 9.5, 6.5 and 5, in solubilised membrane vesicles. Accuracy of the λ_{max} values $\pm$ 5 nm. All PR derived pigments display a strong red-shift upon acidifcation. The pKa of this shift seems to depend on the chromophore, and required further investigation. We did not find a significant effect of the pH in this range on the absorbance band of the GR derived pigments.

According to the ratio A280/A5xx in the absorbance spectra, which varied between 1.5 and 2.5 for all pigments, and the strong band at ~25 kDa for PR (Figure 2.3) and at ~27 kDa for GR (data not shown) observed upon SDS-PAGE analysis, we conclude that a high degree of purification was achieved for all pigments. The purified fractions remained spectrally stable for several weeks at 4°C. Purified PR, PR-DNFS and GR show λ_{max} values of 522 nm, 540 nm and 543 nm with retinal A1 respectively (Figure 2.3), in excellent agreement with literature data and in close agreement with the vesicle data.

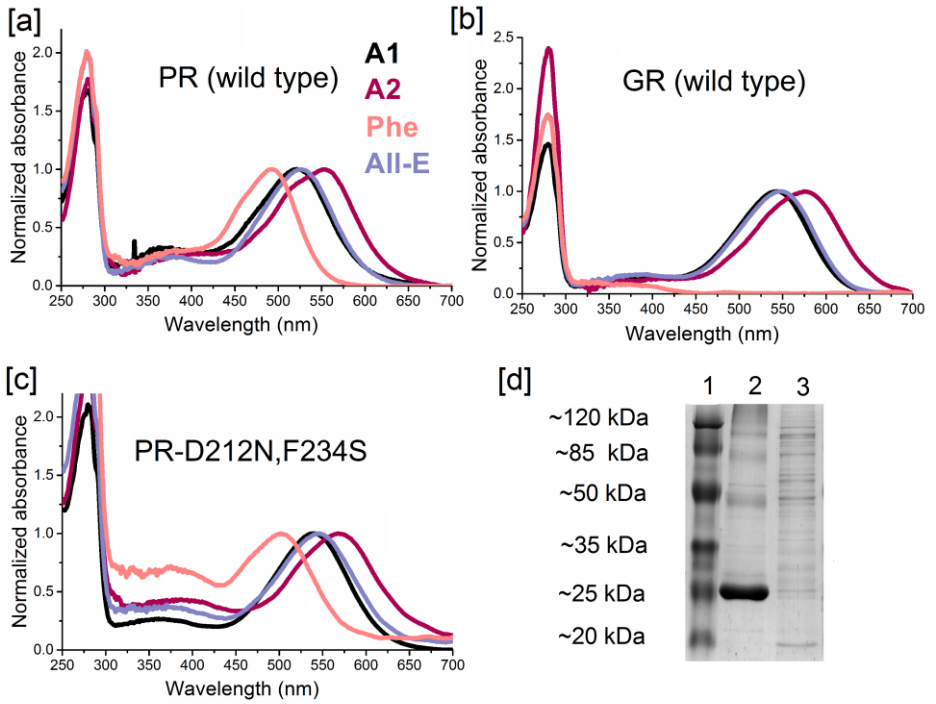

Figure 2.3 Absorbance spectra of purified analog pigments of [a] PR [b] GR and [c] PR-DNFS. No specific peak around 500 nm was obtained for GR with PHE. Spectra are taken at pH 8. Accuracy of the λ_{max} values $\pm$ 2 nm. A1 (black), A2 (magenta), ALL-E (violet) and PHE (pink). [d] Coomassie Blue stained SDS-PAGE gel. The lanes contain (1) protein ladder (2) fraction with purified PR (3) membrane vesicles containing PR. The strong band in lane-2 at ~25 kDa corresponds to the PR monomer.

Incorporation of A2 induces a large red-shift of about 30 nm in the specific absorbance band of all three proteorhodopsins to λ_{max} values of 554 nm, 568 nm and 575 nm for PR, PR-DNFS and GR respectively. In contrast, PHE induces a blue-shift of at least 30 nm in PR and PR-DNFS to 493 nm and 501 nm, respectively. No specific absorbance band was seen for GR purified after incubation with this analog. SDS-PAGE analysis revealed that the opsin was purified successfully, which strengthens our conclusion that the GR opsin is not able to stably bind PHE, or this analog pigment is not stable under our experimental conditions. Incorporation of ALL-E induces a small

red-shift of ~5 nm in all analog pigments to 526 nm, 545 nm and 548 nm for PR, PR-DNFS and GR, respectively. These data are compiled in table 2.2.

2.3.3 Proton pump activity of proteorhodopsins:

While membrane vesicles are economical with respect to ligand usage, we find them less suitable for a quantitative proton-pumping assay. We were not able to isolate vesicle preparations with largely right-side out or inside-out oriented proteorhodopsin. In addition, isolated vesicles can be leaky. Hence, we opted to use intact *E. coli* cells. However, the activity of proteorhodopsins is not easily assayed reproducibly in viable *E. coli* cells. The proton electromotive force is used to drive metabolic processes (e.g. ATP synthesis by ATP synthase) and may trigger the opening of voltage-gated proton channels in the *E. coli* membrane [24]. To avoid such complications, the cells were starved for a few days, with most reproducible results obtained after 4-5 days of starvation. The proton pump activity of the native proteorhodopsins and their analog pigments was measured in starved cell suspensions in the presence of the K^+ ionophore valinomycin and potassium ions, which eliminates the electrical component of the electrochemical proton gradient. This allows quantification of the proton efflux mediated by the proteorhodopsins, without interference from any possible back-pressure effects of the transmembrane electrical potential gradient. For the cells producing proteorhodopsin, this was seen as a decrease in pH upon illumination, which slowly returned to the baseline value in darkness. We did not try to optimize conditions to achieve maximal pumping rates (spectral range, photon intensity, vesicle density). Instead, for mutual comparison, the calculated rates were normalized relative to the most active A1 rhodopsin (GR).

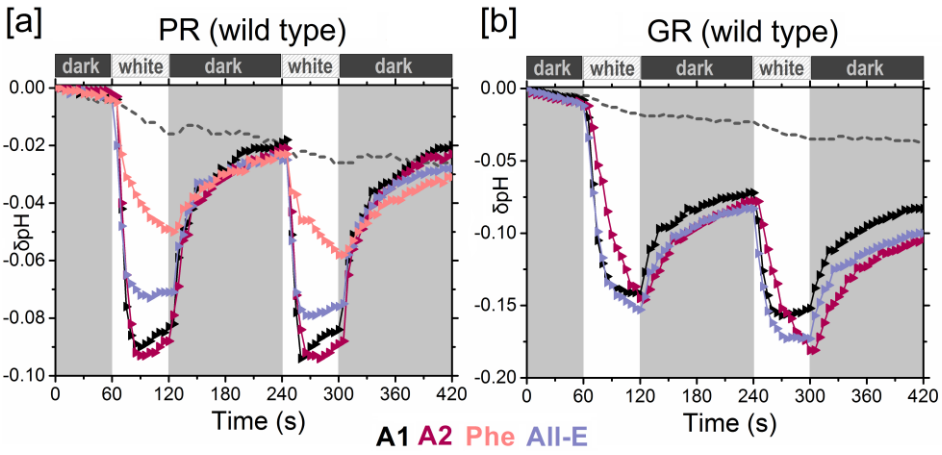

Figure 2.4 Proton pumping traces of starved *E. coli* UT5600 cell suspensions containing PR/GR or one of its analogs. A1 (black), A2 (magenta), ALL-E (violet) and PHE (pink). Dotted black line represents the control opsin without a retinal.

Representative traces for PR and GR and their analog pigments are shown in Figure 2.4, and the normalized pumping rates in Table 2.2. The highest pumping rates obtained with A1 were observed for GR (4-5 protons mol^{-1} s^{-1}), which corroborates findings from previous studies [18, 22, 25]. The lowest pumping activity of was observed for PR-DNFS, which retains 40-60% pumping activity of the wild type. This is consistent with previous data using sphaeroplast suspensions [1]. Interestingly, with A2 or ALL-E, all three proteorhodopsins presented proton pump activity very similar to that with A1, indicating that these analogs hardly perturb the proton translocation mechanism. Also, PHE retains significant proton pump activity for both PR and PR-DNFS. Light induced pH changes were largely prevented by the addition of 40 µM of the protonophorous uncoupler CCCP. In addition, no light induced pH changes were observed for the control situation, where the opsin-expression was not induced but retinal was present (data not shown), or the converse, i.e. when the opsin was expressed but retinal not added (Figure 2.4).

Species	Retinal analog	λmax (nm)	Spectral shift (nm)	Spectral shift (cm^{-1})	Pump rate
PR	A1	522	NA	NA	++
	A2	554	+32	1106	++
	ALL-E	526	+4	146	++
	PHE	493	-29	1127	++
PR-DNFS	A1	540	NA	NA	+
	A2	568	+28	913	+
	ALL-E	545	+5	170	+
	PHE	501	-39	1442	+
GR	A1	543	NA	NA	+++
	A2	575	+32	1025	+++
	ALL-E	548	+5	168	+++

Table 2.2 Proton pumping scores and absorbance maximum values of PR, PR-DNFS, GR and their analogs. GR does not form a stable pigment with PHE. The λ_{max} of the purified proteins were measured at pH 8, with an accuracy of $\pm$ 2 nm (n=3). The spectral shift relative to A1 is given in wavelength (nm) and energy (cm^{-1}). Proton pumping rates were normalized with respect to GR with retinal A1. +++ pumping rate 70-120 % of that of A1-GR ; ++ pumping rate 40-70 % of that of A1-GR; + pumping rate 20-40 % of that of A1-GR

2.3.4 Homology models of PR and GR:

In order to evaluate the effect of retinal analogs and mutations, a 3D structure of PR and GR would be very useful. However, a crystal structure is not available for these retinal proteins and the PR structure solved using NMR spectroscopy [26] significantly deviates even in the transmembrane domain from the crystal structures of other microbial retinal proteins [27, 28] and from earlier PR homology models based on the bR structure [29, 30]. Hence, we decided to generate homology models for GR and PR, based upon the crystal structures of retinal proteins with which they had the highest sequence identity at that time (XR and SRII respectively).

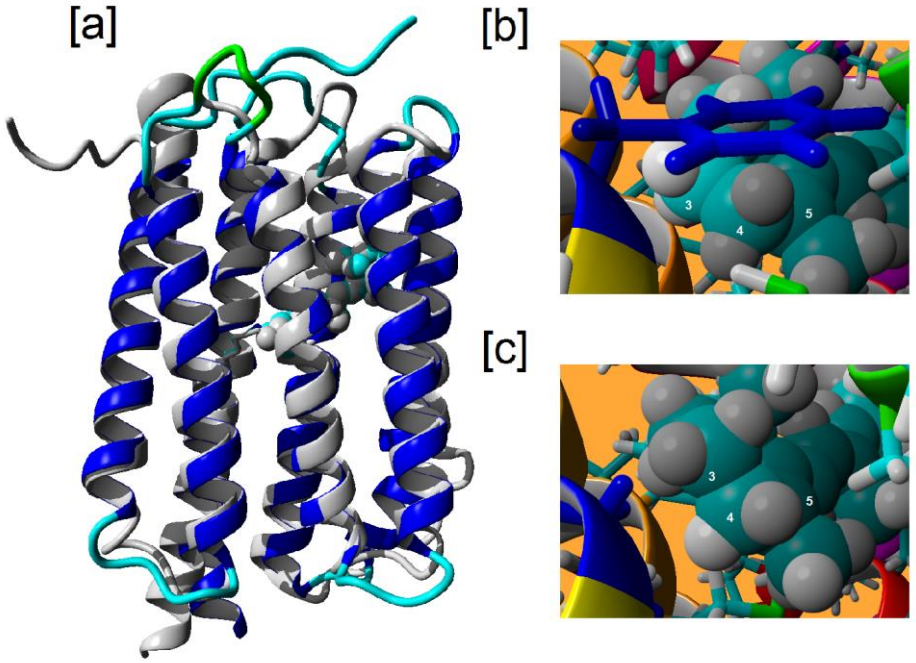

Figure 2.5 Homology models of PR and GR. [a] Overlay of the backbone of the PR homology model (blue) with that of the BPR structure [23] (PDB: 4KNF; grey). Retinal is represented in cyan as a space filled residue. [b] and [c] Enlarged view of the binding pocket in the PR [b] and GR [c] homology models showing the sites Phe152 (PR) and Gly172 (GR) in dark blue. Retinal is represented as in [a] with some ring carbons numbered.

The resulting models for PR and GR show high similarity in the structure of the transmembrane domain and the binding pocket, but, as expected, show variation in the loop regions. Recently, a crystal structure was published for BPR having 83% sequence identity with PR [27]; (PDB 4KNF). A comparison of this structure with our homology model for PR, presented in Figure 2.5, shows excellent conformity in the α-helical domain, and a root-mean-square deviation of only 1.8 Å over all identical residues.

2.4 Discussion

2.4.1 Proteorhodopsin selection

PR, and to a smaller extent GR have been extensively characterized with their native ligand A1. We obtained good expression levels in the *E. coli* strain UT5600 (at least 10 mg/L for PR and 4 mg/L for GR). The produced proteorhodopsins could be purified to a high degree. Furthermore, we obtained good agreement between the λ_{max} values obtained from the absorbance spectra of the purified protein, and the difference spectrum obtained after bleaching the solubilized membrane vesicles with hydroxylamine.

The spectral characteristics of a retinylidene chromophore are strongly affected by its interaction with protein residues lining its binding pocket. However, residues can also exert their effect on the chromophore from a distance, via their involvement in the secondary structure of the protein or their contribution to the local electrostatic field. This is exemplified in the D212N,F234S double mutant of PR, which has been previously described [1]. The authors report that mutation of the binding pocket residue Phe234 to Ser causes a red-shift of the main absorbance band and strongly reduces proton pump activity. According to our homology model, residue Asp212 is located in interhelical loop E-3 and it is not surprising that the single mutation D212N does not change the absorbance or pumping activity of PR (data not shown). However, when these mutations are combined, this yields a red-shifted PR-DNFS that retains significant proton pump activity. We could fully reproduce these characteristics and included this double mutant in our study to test whether spectral shifts induced by a mutation are complementary to those implemented by retinal analogs. With PR-DNFS, expression yields of at least 6 mg/L culture were obtained.

2.4.2 Analog pigments

To our knowledge no detailed study has been reported to date on the effect of retinal analogs on molecular properties of PR or GR. In the context of a wide-angle X-ray scattering study of PR, the 13-desmethyl,13-iodo retinal A1 analog was tested and shown to induce a 23 nm red-shift [30]. In the current study, we focus on ring modifications.

Incorporation of A2 is expected to red-shift the absorbance band relative to A1. This has been demonstrated previously in archaeal and channel rhodopsins (ChR), where red-shifts of about 30 nm are reported, with only a small effect on proton pumping or channel functionality [2-5], as well as in XR with a 23 nm red-shift [9]. As anticipated, this analog rapidly reacted to completeness with all three proteo-opsins and induced comparable red-shifts of about 30 nm corresponding to an energy difference of about 1100 cm^{-1} (Table 2.1). The resulting A2 analog pigments were quite stable in detergent solution and could be purified to a high degree. The A2 analog pigments also present a slightly broadened absorbance band with a small shoulder at the hypsochromic wing of the spectrum (at about 510 nm for PR and about 530 nm for the other two analog pigments). Such a shoulder was previously observed in the A2 analogs of bR [26], ChR and AR3 [29]. Most likely, this shoulder represents fine structure of vibronic origin, possibly due to a more rigid conformation [6], e.g. also evident in the spectrum of ALL-E (see Appendix). An important observation is that A2 is largely equivalent to A1 in maintaining proton pump activity in all three proteorhodopsins (Figure 2.4, Table 2.2).

In ALL-E, the polyene system is locked in the 6-s-*trans* configuration effectuating optimal conjugation. This analog was previously tested on bacterio-opsin and xantho-opsin, to study the effect of the configuration about the C6-C7 single bond [6, 11]. It was observed that the 6-s-*trans* form

of this compound smoothly reacted with both opsins, but the 6-s-*cis* form did not. The 6-s-*trans* analog provided spectral properties very similar to native bR and XR, and retained 90% of the bR pumping activity. This corroborated previous solid-state NMR studies indicating that retinal A1 has taken up a 6-s *trans* configuration upon binding to bacterio-opsin [31]. The transition from the twisted 6-s-*cis* in the free retinal A1 to the planar 6-s-*trans* form in the binding pocket of the protein accounts for a part of the spectral shift in the binding site. In ALL-E , the 6-s-*trans* form already has been enforced, which explains its red-shifted absorbance band relative to free retinal A1 (Appendix A.2) and its small effect on the absorbance band when bound in bR or XR. ALL-E was not tested before on PR or GR. This analog reacted with all three proteo-opsins, reaching completion in 30-60 min at RT. The resulting analog pigments exhibit only small red-shifts relative to the native pigments (4-5 nm). These data present strong evidence that in eubacterial rhodopsins, the retinal is bound in the 6-s-*trans* configuration, as well. This implies that the bathochromic shift of the absorbance band in XR and archaerhodopsins, relative to these eubacterial rhodopsins, is largely induced by the protein environment. All three proteorhodopsin analogs containing ALL-E retained 70-100% proton pump activity (Table 2.2). This would render this retinal analog interesting for optogenetic applications. It can be supplied directly or in precursor form in the diet and will hardly interfere with the visual system. In addition, it may be less prone to generate metabolic products like retinoic acids with strong signalling function.

PHE was previously reported to react very slowly with bacterio-opsin yielding a strongly blue-shifted analog pigment [7, 8]. In case of the eubacterial opsins, PHE behaves quite differently from the other two analogs. It forms a stable pigment with the PR and PR-DNFS opsins, but not with the GR opsin. Furthermore, it regenerates the PR opsins slowly, with only partial regeneration after 60 min incubation at RT, requiring

additional overnight incubation at 4°C. Finally, it induced a significant blue-shift in absorbance, compared to A1. The slow regeneration is most likely due to a poor fit in the opsin binding pocket because of the absence of the methyl groups on the ring element, which sterically contribute to correct positioning and stabilization of the ring and to its interaction with its protein environment [6, 32]. Nevertheless, the resulting analog pigments maintained significant proton pump activity and could be successfully purified.

The structural models we generated for GR and PR may present a clue for their different reactivity with PHE. Figure 2.5 shows the models for the rear end of the binding pockets. The most striking difference is seen at the position of Phe152 in PR, where GR has a glycine residue (Gly178). This difference is physiologically relevant, since it was demonstrated that mutating Gly178 in GR to a bulkier Trp abolished strong binding of the carotenoid echinenone, which is involved in energy transfer to the retinal [18, 33, 34], and eliminated this energy transfer. The smaller Gly residue at position 178 apparently is required to allow enough space for immobilizing the carotenoid ring [6, 16], thereby allowing energy transfer and increasing the cross section for photo-activation of retinal. We surmise that the aromatic ring of Phe152 in PR, which is positioned right above the ring element of retinal, would contribute significant π-π stacking interaction. Together with the methyl groups on the polyene chain, this may sufficiently stabilize PHE in the binding pocket. GR cannot provide this stacking interaction, and thus may not provide sufficient interaction energy or too much motional freedom for the PHE to form a stable protonated Schiff base. This hypothesis can be verified by testing whether the G178F mutant of GR will yield a stable pigment with PHE.

In this context, a comparison with XR, is appropriate, since XR also binds a carotenoid (salinixanthin, a derivative of echinenone) [35]. The position

equivalent to Gly178 in GR carries the same residue in XR (Gly156). Xantho-opsin is reported to slowly react with PHE in the presence of bound salinixanthin, generating a stable pigment [30]. Possibly, the presence of the carotenoid ring sufficiently stabilizes PHE in the binding pocket. Since there is no echinenone available in our *E. coli* expression system, it needs to be investigated whether complementation with echinenone would result in a stable analog pigment of GR with PHE. It has been suggested that carotenoid fixation is required for pigment formation in XR [6, 36]. Our results show that this is not the case for GR, which easily generates analog pigments that retain full proton pumping capacity.

2.5 Conclusion

Our results demonstrate that ring modification can affect the affinity of the analog for the retinal binding site and will usually modulate the spectral properties of the respective rhodopsin, but, importantly, can largely maintain proton pump activity. This presents good prospects for further modification trials in the ring and eventual biotechnological applications. The smooth reaction with ALL-E while implementing only a small red-shift, corroborates available evidence, that the retinal chromophore in eubacterial rhodopsins is also bound in the 6-s-*trans* configuration. We further show that the spectral shifts effectuated by the analogs can be additive to spectral shifts induced by mutagenesis. Hence, combining selected mutagenesis with ligand analogs offers promising prospects for further extending the wavelength range of rhodopsins.

References

[1] Kim, S. Y., Waschuk, S. A., Brown, L. S. and Jung, K. H. "Screening and characterization of proteorhodopsin color-tuning mutations in Escherichia coli with endogenous retinal synthesis", *Biochim Biophys Acta*, 2008. **1777**(6): p. 504-13.

[2] Tokunaga, F. and Ebrey, T. "The blue membrane: The 3-dehydroretinal-based artificial pigment of the purple membrane ", *Biochemistry*, 1978. **17**(10): p. 1915-1922.

[3] Spudich, J. L., McCain, D. A., Nakanishi, K., Okabe, M., Shimizu, N., Rodman, H., Honig, B. and Bogomolni, R. A. "Chromophore/protein interaction in bacterial sensory rhodopsin and bacteriorhodopsin ", *Biophys J*, 1986. **49**(2): p. 479-83.

[4] Iwasa, T. "Artificial pigments of halorhodopsin and their chloride pumping activities ", *Biochemistry*, 1992. **31**(4): p. 1190-5.

[5] Sineshchekov, O. A., Govorunova, E. G., Wang, J. and Spudich, J. L. "Enhancement of the long-wavelength sensitivity of optogenetic microbial rhodopsins by 3,4-dehydroretinal ", *Biochemistry*, 2012. **51**(22): p. 4499-506.

[6] Smolensky Koganov, E., Hirshfeld, A. and Sheves, M. "Retinal beta-ionone ring-salinixanthin interactions in xanthorhodopsin: a study using artificial pigments ", *Biochemistry*, 2013. **52**(7): p. 1290-301.

[7] Derguini, F., Bigge, C. F., Croteau, A. A., Balogh-Nair, V. and Nakanishi, K. "Visual pigments and bacteriorhodopsins formed from aromatic retinal analogs ", *Photochem Photobiol*, 1984. **39**(5): p. 661-5.

[8] Maeda, A., Asato, A. E., Liu, R. S. and Yoshizawa, T. "Interaction of aromatic retinal analogues with apopurple membranes of Halobacterium halobium ", *Biochemistry*, 1984. **23**(11): p. 2507-13.

[9] Smolensky, E. and Sheves, M. "Retinal-salinixanthin interactions in xanthorhodopsin: a circular dichroism (CD) spectroscopy study with artificial pigments ", *Biochemistry*, 2009. **48**(34): p. 8179-88.

[10] Steen, R. v. d., Biesheuvel, P. L., Mathies, R. A. and Lugtenburg, J. "Retinal analogs with locked 6-7 conformations show that bacteriorhodopsin requires the 6-s-*trans* conformation of the chromophore ", *J Am Chem Soc*, 1986. **108**(20): p. 6410-6411.

[11] van Wijk, Arjan A. C., van de Weerd, Michiel B. and Lugtenburg, J. "Synthetic scheme for the preparation of ^{13}C-labeled 3,4-didehydro-retinal, 3-hydroxyretinal, and 4-hydroxyretinal up to uniform ^{13}C-enrichment ", *E J Org Chem*, 2003. **2003**(5): p. 863--868.

[12] Hubbard, R., Brown, P. K. and Bownds, D. "243: Methodology of vitamin A and visual pigments ", *Methods Enzymol*, 1971. **18, Part C**: p. 615 - 653.

[13] Groenendijk, G. W., Jansen, P. A., Bonting, S. L. and Daemen, F. J. "Analysis of geometrically isomeric vitamin A compounds ", *Methods Enzymol*, 1980. **67**: p. 203-20.

[14] Friedrich, T., Geibel, S., Kalmbach, R., Chizhov, I., Ataka, K., Heberle, J., Engelhard, M. and Bamberg, E. "Proteorhodopsin is a light-driven proton pump with variable vectoriality ", *J Mol Biol*, 2002. **321**(5): p. 821-38.

[15] Gordeliy, V. I., Labahn, J., Moukhametzianov, R., Efremov, R., Granzin, J., Schlesinger, R., Buldt, G., Savopol, T., Scheidig, A. J., Klare, J. P. and Engelhard, M. "Molecular basis of transmembrane signalling by sensory rhodopsin II-transducer complex ", *Nature*, 2002. **419**(6906): p. 484-7.

[16] Luecke, H., Schobert, B., Stagno, J., Imasheva, E. S., Wang, J. M., Balashov, S. P. and Lanyi, J. K. "Crystallographic structure of xanthorhodopsin, the light-driven proton pump with a dual chromophore ", *Proc Natl Acad Sci U S A*, 2008. **105**(43): p. 16561-5.

[17] Dioumaev, A. K., Brown, L. S., Shih, J., Spudich, E. N., Spudich, J. L. and Lanyi, J. K. "Proton transfers in the photochemical reaction cycle of proteorhodopsin ", *Biochemistry*, 2002. **41**: p. 5348-5358.

[18] Miranda, M. R., Choi, A. R., Shi, L., Bezerra, A. G., Jr., Jung, K. H. and Brown, L. S. "The photocycle and proton translocation pathway in a cyanobacterial ion-pumping rhodopsin", *Biophys J*, 2009. **96**(4): p. 1471-81.

[19] Yaowu, X., Ranga, P., Richard, K. and and Mark, B. "Time-resolved FTIR spectroscopy of the photointermediates involved in fast transient H^+ release by Proteorhodopsin", *J Phys Chem B*, 2005. **109**(1): p. 634-641.

[20] Béjà, O., Aravind, L., Koonin, E. V., Suzuki, M. T., Hadd, A., Nguyen, L. P., Jovanovich, S. B., Gates, C. M., Feldman, R. A., Spudich, J. L., Spudich, E. N. and DeLong, E. F. "Bacterial rhodopsin: Evidence for a new type of phototrophy in the sea", *Science*, 2000. **289**(5486): p. 1902-1906.

[21] Dioumaev, A. K., Wang, J. M., Balint, Z., Varo, G. and Lanyi, J. K. "Proton transport by proteorhodopsin requires that the retinal Schiff base counterion Asp-97 be anionic", *Biochemistry*, 2003. **42**(21): p. 6582-7.

[22] Vogt, A., Wietek, J. and Hegemann, P. "Gloeobacter rhodopsin, limitation of proton pumping at high electrochemical load", *Biophys J*, 2013. **105**(9): p. 2055-63.

[23] Choi, A. R., Shi, L., Brown, L. S. and Jung, K. H. "Cyanobacterial light-driven proton pump, Gloeobacter rhodopsin: complementarity between rhodopsin-based energy production and photosynthesis", *PLoS One*, 2014. **9**(10): p. e110643.

[24] Wang, W. W., Sineshchekov, O. A., Spudich, E. N. and Spudich, J. L. "Spectroscopic and photochemical characterization of a deep ocean proteorhodopsin", *J Biol Chem*, 2003. **278**(36): p. 33985-91.

[25] Lee, K. A. and Jung, K.-H. "ATP regeneration system using *E. coli* ATP synthase and *Gloeobacter* rhodopsin and its stability", *J Nanosci Nanotechnol*, 2011. **11**(5): p. 4261-4264.

[26] Reckel, S., Gottstein, D., Stehle, J., Lohr, F., Verhoefen, M. K., Takeda, M., Silvers, R., Kainosho, M., Glaubitz, C., Wachtveitl, J., Bernhard, F., Schwalbe, H., Guntert, P. and Dotsch, V. "Solution NMR structure of proteorhodopsin", *Angew Chem Int Ed Engl*, 2011. **50**(50): p. 11942-6.

[27] Ran, T., Ozorowski, G., Gao, Y., Sineshchekov, O. A., Wang, W., Spudich, J. L. and Luecke, H. "Cross-protomer interaction with the photoactive site in oligomeric proteorhodopsin complexes", *Acta Crystallogr D Biol Crystallogr*, 2013. **69**(10): p. 1965-80.

[28] Bamann, C., Bamberg, E., Wachtveitl, J. and Glaubitz, C. "Proteorhodopsin", *Biochim Biophys Acta*, 2014. **1837**(5): p. 614-25.

[29] Rupenyan, A., van Stokkum, I. H., Arents, J. C., van Grondelle, R., Hellingwerf, K. and Groot, M. L. "Characterization of the primary photochemistry of proteorhodopsin with femtosecond spectroscopy", *Biophys J*, 2008. **94**(10): p. 4020-30.

[30] Malmerberg, E., Omran, Z., Hub, J. S., Li, X., Katona, G., Westenhoff, S., Johansson, L. C., Andersson, M., Cammarata, M., Wulff, M., van der Spoel, D., Davidsson, J., Specht, A. and Neutze, R. "Time-resolved WAXS reveals accelerated conformational changes in iodoretinal-substituted proteorhodopsin", *Biophys J*, 2011. **101**(6): p. 1345-53.

[31] Harbison, G. S., Smith, S. O., Pardoen, J. A., Courtin, J. M., Lugtenburg, J., Herzfeld, J., Mathies, R. A. and Griffin, R. G. "Solid-state ^{13}C NMR detection of a perturbed 6-s-*trans* chromophore in bacteriorhodopsin", *Biochemistry*, 1985. **24**(24): p. 6955-62.

[32] Sheves, M., Friedman, N., Rosenbach, V. and Ottolenghi, M. "Preparation of (1,1,5-tri-demetyl)bacteriorhodopsin pigment and its photocycle study", *FEBS Letters*, 1984. **166**(2): p. 245--247.

[33] Imasheva, E. S., Balashov, S. P., Choi, A. R., Jung, K. H. and Lanyi, J. K. "Reconstitution of *Gloeobacter violaceus* rhodopsin with a light-harvesting carotenoid antenna", *Biochemistry*, 2009. **48**(46): p. 10948-55.

[34] Balashov, S. P., Imasheva, E. S., Choi, A. R., Jung, K. H., Liaaen-Jensen, S. and Lanyi, J. K. "Reconstitution of gloeobacter rhodopsin with echinenone: role of the 4-keto group", *Biochemistry*, 2010. **49**(45): p. 9792-9.

[35] Balashov, S. P., Imasheva, E. S., Boichenko, V. A., Anton, J., Wang, J. M. and Lanyi, J. K. "Xanthorhodopsin: a proton pump with a light-harvesting carotenoid antenna", *Science*, 2005. **309**(5743): p. 2061-4.

[36] Imasheva, E. S., Balashov, S. P., Wang, J. M., Smolensky, E., Sheves, M. and Lanyi, J. K. "Chromophore interaction in xanthorhodopsin--retinal dependence of salinixanthin binding", *Photochem Photobiol*, 2008. **84**(4): p. 977-84.